

A study on the squeezing hydrodynamics of a lubricant between two rough parallel plates: Hip-Joint representation

Hemangini R. Jani¹, H. C. Patel², and G. M. Deheri³

¹Ph. D. Section,
Gujarat Technology University,
Ahmedabad, Gujarat, India

²Gujarat University,
Ahmedabad, Gujarat, India

³Department of Mathematics,
Sardar Patel University V. V. Nagar,
Anand, Gujarat, India

Copyright © 2016 ISSR Journals. This is an open access article distributed under the *Creative Commons Attribution License*, which permits unrestricted use, distribution, and reproduction in any medium, provided the original work is properly cited.

ABSTRACT: The unsteady squeezing hydrodynamics of lubrication between two rough parallel plates is analyzed here, which can be modified to represent a hip-joint, where in different moments can be numerically modelled. The stochastic model of Christensen and Tonder has been deployed here to evaluate the effect of surface roughness. Also the effect of roughness parameters on different moments is numerically modelled. The associated stochastically averaged Reynolds equation is solved to obtain the pressure distribution. The results obtained here are presented in graphical forms. The graphical representation establishes that the standard deviation associated with roughness has significant impact. Further it is observed that the situation remains relatively better in the case of negatively skewed roughness. This effect advances when variance (-ve) occurs.

KEYWORDS: Squeezing motion, Fluid equation, hydrodynamic lubricant, magnetic field, Hip-joint, Reynolds equation.

1 INTRODUCTION

Since the beginning of civilization, man has been trying to understand the nature around him. Because of curiosity and continuous enhancement of knowledge, he has been involved in unveiling the mysteries of the universe. He has been trying to understand the origin of life itself and the mechanisms involved in making the life self-sustaining in an adequately optimized manner. From such curiosity and continuous enhancement of knowledge rises the Biomechanics which involves mechanics as well as biology [1].

One of the most important biomechanical system is the human body itself, where the synovial joints play an essential role during motion. In fact Bio-tribology may be defined as the science of lubrication, friction and wear of a biomechanical system involving two surfaces in relative motion and separated by a very thin fluid film, [Dowson and Wright (1973)][2]. Here the emphasis has been given only to those aspects of synovial joints which can be investigated on the basis of hydrodynamic lubrication theory.

The hip joint is a complex biological system. It is a synovial joint whose main component is synovial fluid. The synovial fluid provides lubrication between the femur and acetabulum, both of which are covered with hyaline cartilage; it also provides nutrients for the other joint components. Deterioration of the hip joint has led to the development of artificial hip joints. The most popular system in use today is the metal-on-metal hip implants UHMWPE system. In recent years, the focus

of research has switched over to improve the longevity of the implant; because younger patients require total hip replacements. This has led to increased use of ceramic-on-ceramic, as well as second generation metal-on-metal bearing systems and the use of hip-resurfacing techniques. These bearing systems are known to have problems due to the large amount of revision surgeries required. A better knowledge of the bio-tribological aspects of the artificial hip implant can help in the understanding and ultimate improvement of the prostheses.

Reference [3] analyzed the fluid film lubrication in artificial hip joint replacements with surface of high elastic modulus. Lubrication mechanics and contact mechanics were investigated for total hip-joint replacement made from hard bearing surfaces such as metal on metal, ceramic on ceramic and polyethylene against the hard bearing surface. The most important factor effecting the lubrication film thickness was found to be the radial clearance between the ball and socket. Practical consideration of manufacturing the hard bearing surface were also discussed.

Reference [4] studied the effect of bearing geometry and structure support on transient elastohydrodynamic lubrication of metal on metal hip implants. This investigation can be improved through the optimization of bearing geometry in term of a small clearance and the structural support such as a polyethylene backing under neath a metallic bearing in a sandwich acetabula cup form. Further the result showed that a larger lubricant film due to the polyethylene backing could be significantly enhance by the transient squeeze film action.

Reference [5] deliberate contact mechanics and elastohydrodynamic lubrication in a novel metal on metal hip implant with an aspherical bearing surface. Alpherabola, as the acetabular surface was investigated for both contact mechanics and elastohydrodynamic lubrication under steady state condition. When compared with conventional spherical bearing surfaces, a more uniform pressure distribution and a thickness within the loaded conjunction were predicted for this novel Alpherabola hip implant.

Reference [6] reviewed the literature concerned with lubrication and wear modelling of artificial hip-joints.

A steady state numerical model was extended by reference [7] with dynamic experimental data for hard-on-hard bearing used total hip replacements to verify the tribological relevance. Lubrication regimes were shown to depend strongly on the Kinematics loading conditions.

Francesca Di Puccio and Lorenza Mattei from reference [8] worked in Bio-tribology of artificial hip joint. Discussed artificial hip joints, defining materials and geometric properties examining their friction, lubrication and wear characteristics. This study highlighted how the friction, lubrication and wear were interconnected.

Here it has been proposed to study and analyze the squeezing hydrodynamics of a lubricant between two rough parallel plates in the context of hip-joint replacement.

2 ANALYSIS

2.1 REYNOLDS TRANSPORTATION THEOREM

It is well-known that The Eulerian coordinate system is a more appropriate system to describe the path of the particles for fluid mechanics. The fundamental laws of mechanics, which are conservation of mass, momentum and energy ,are expressed in Lagrangian coordinates required to be convert them Eulerian coordinates using the Reynolds Transportation theorem:

$$\frac{D}{Dt} \int_{V(t)} \phi \delta V = \int_{V(t)} \left\{ \frac{\partial \phi}{\partial t} + \frac{\partial(\phi u_j)}{\partial x_j} \right\} \delta V \tag{1}$$

The details regarding this equation can be had from (Ramjee 2009) [9]

With usual assumptions of fluid film lubrication the velocity profiles are governed by [9]

$$\int_0^{h(x_1, x_2, t)} u_1(x_1, x_2, x_3, t) \partial x_3 = -\frac{\partial p}{\partial x_1} \frac{h^3}{12\mu} + \frac{U_1 h}{2} \tag{2}$$

$$\int_0^{h(x_1, x_2, t)} u_2(x_1, x_2, x_3, t) \partial x_3 = -\frac{\partial p}{\partial x_2} \frac{h^3}{12\mu} + \frac{U_2 h}{2}$$

where μ = viscosity of lubricant.

In view of roughness characteristic and stochastic modelling of [10],[11],[12]. So equation (2) transform to

$$\int_0^{h(x_1, x_2, t)} u_1(x_1, x_2, x_3, t) dx_3 = -\frac{\partial p}{\partial x_1} \frac{G(h)}{12\mu} + \frac{U_1 h}{2}$$

$$\int_0^{h(x_1, x_2, t)} u_2(x_1, x_2, x_3, t) dx_3 = -\frac{\partial p}{\partial x_2} \frac{G(h)}{12\mu} + \frac{U_2 h}{2}$$
(3)

Where $G(h) = h^3 + 3\sigma^2 h + 3\alpha^2 h + 3\alpha h^2 + 3\sigma^2 \alpha + \alpha^3 + \varepsilon$

σ = standard deviation, α = variance, ε = skewness

In view of the boundary conditions, $u_1(x_1, x_2, x_3, t) = U_1$ and $u_2(x_1, x_2, x_3, t) = U_2$

One obtains,

$$\int_0^{h(x_1, x_2, t)} \frac{\partial u_3}{\partial x_3} dx_3 = -\frac{\partial}{\partial x_1} \left\{ -\frac{\partial p}{\partial x_1} \frac{G(h)}{12\mu} + \frac{U_1 h}{2} \right\} + U_1 \frac{\partial h}{\partial x_1} - \frac{\partial}{\partial x_2} \left\{ -\frac{\partial p}{\partial x_2} \frac{G(h)}{12\mu} + \frac{U_2 h}{2} \right\} + U_2 \frac{\partial h}{\partial x_2}$$

$$= \frac{\partial}{\partial x_1} \left\{ \frac{G(h)}{12\mu} \frac{\partial p}{\partial x_1} \right\} - \frac{U_1}{2} \frac{\partial h}{\partial x_1} + U_1 \frac{\partial h}{\partial x_1} + \frac{\partial}{\partial x_2} \left\{ \frac{G(h)}{12\mu} \frac{\partial p}{\partial x_2} \right\} - \frac{U_2}{2} \frac{\partial h}{\partial x_2} + U_2 \frac{\partial h}{\partial x_2}$$
(4)

So, one arrives at

$$U_3 - \frac{U_1}{2} \frac{\partial h}{\partial x_1} - \frac{U_2}{2} \frac{\partial h}{\partial x_2} = \frac{\partial}{\partial x_1} \left\{ \frac{G(h)}{12\mu} \frac{\partial p}{\partial x_1} \right\} + \frac{\partial}{\partial x_2} \left\{ \frac{G(h)}{12\mu} \frac{\partial p}{\partial x_2} \right\}$$
(5)

Using Kinematic boundary conditions on the surface $x_3 = h$, one leads to

$$U_3 = \frac{\partial h}{\partial t} + U_1 \frac{\partial h}{\partial x_1} + U_2 \frac{\partial h}{\partial x_2}$$
(6)

Substitution of (6) in (5) results in

$$\frac{\partial}{\partial x_1} \left\{ \left(\frac{G(h)}{12\mu} \right) \frac{\partial p}{\partial x_1} \right\} + \frac{\partial}{\partial x_2} \left\{ \left(\frac{G(h)}{12\mu} \right) \frac{\partial p}{\partial x_2} \right\} = \frac{\partial h}{\partial t} + \frac{U_1}{2} \frac{\partial h}{\partial x_1} + \frac{U_2}{2} \frac{\partial h}{\partial x_2}$$

In general form this can be written as,

$$\nabla \cdot \left(\frac{G(h)}{12\mu} \nabla P \right) = \nabla \cdot \left(\frac{h \vec{U}}{2} \right) + \frac{\partial h}{\partial t}$$
(7)

where \vec{U} is the surface velocity vector.

2.2 REYNOLDS EQUATION APPLIED TO A HIP-JOINT

Some assumptions are made to model the Hip-Joint which are,

- 1) The fluid is iso-viscous (Newtonian)
- 2) The cup is positioned horizontally
- 3) Walking cycle imposed is based on the Bergmann walking cycle

Synovial fluid and blood plasma are known to have non-Newtonian fluid properties, however studies have concluded that at high shear rates, an iso-viscous assumption is valid. The ace tabular cup is anatomically positioned at 45°; however the contact mechanics allow for the model to be developed in a horizontal position. The Bergmann walking cycle consists of a loading pattern which is double-peaked. This has resulted from studies conducted by Bergmann et al. (1995)[13] on the influence of heel strike on the loading of the hip joint. The coordinate system that would best describe the hip joint would be the spherical coordinate system, Thus expanding equation (7) in spherical coordinates,

For Left Hand Side of (7) one concludes that

$$\nabla P = \frac{\partial P}{\partial R} \hat{R} + \frac{1}{R} \frac{\partial P}{\partial \theta} \hat{\theta} + \frac{1}{R \sin \theta} \frac{\partial P}{\partial \phi} \hat{\phi}$$

where in R is the radius of the acetabular cup so that,

$$\frac{\partial P}{\partial R} = 0$$

(because P is normal stress, it is scalar and R is fixed here)

Making use of divergence formula for spherical coordinates one conclude that

$$\therefore \nabla \cdot \left(\frac{G(h)}{12\mu} \nabla P \right) = \frac{1}{R^2} \left\{ \frac{1}{\sin \theta} \frac{\partial}{\partial \theta} \left(\frac{G(h)}{12\mu} \sin \theta \frac{\partial P}{\partial \theta} \right) + \frac{1}{\sin^2 \theta} \frac{\partial}{\partial \phi} \left(\frac{G(h)}{12\mu} \frac{\partial P}{\partial \phi} \right) \right\} \quad (8)$$

For RHS of equation (7) one derives that

$$\nabla \cdot \left(\frac{h\vec{U}}{2} \right) = \frac{1}{2R\sin\theta} \left[h \cos \theta U_\theta + h \sin \theta \frac{\partial U_\theta}{\partial \theta} + U_\theta \sin \theta \frac{\partial h}{\partial \theta} + h \frac{\partial U_\phi}{\partial \phi} + U_\phi \frac{\partial h}{\partial \phi} \right] \quad (9)$$

Substituting the values of (8) and (9) in (7), one arrives at

$$\frac{1}{R^2} \left\{ \frac{1}{\sin \theta} \frac{\partial}{\partial \theta} \left(\frac{G(h)}{12\mu} \sin \theta \frac{\partial P}{\partial \theta} \right) + \frac{1}{\sin^2 \theta} \frac{\partial}{\partial \phi} \left(\frac{G(h)}{12\mu} \frac{\partial P}{\partial \phi} \right) \right\} = \frac{1}{2R\sin\theta} \left[h \cos \theta U_\theta + h \sin \theta \frac{\partial U_\theta}{\partial \theta} + U_\theta \sin \theta \frac{\partial h}{\partial \theta} + h \frac{\partial U_\phi}{\partial \phi} + U_\phi \frac{\partial h}{\partial \phi} \right] + \frac{\partial h}{\partial t} \quad (10)$$

where the surface velocity components, U_θ and U_ϕ are given by:

$$U_\theta = -R\omega_{x_1} \sin \phi + R\omega_{x_2} \cos \phi$$

$$U_\phi = -R\omega_{x_1} \cos \phi \cos \theta - R\omega_{x_2} \sin \phi \cos \theta + R\omega_{x_3} \sin \phi + R\omega_{x_3} \sin \theta$$

Substituting these relations into equation (10) and simplifying, one comes across

$$\begin{aligned} & \sin \theta \frac{\partial}{\partial \theta} \left(G(h) \sin \theta \frac{\partial p}{\partial \theta} \right) + \frac{\partial}{\partial \phi} \left(G(h) \frac{\partial p}{\partial \phi} \right) \\ &= 6\mu R^2 \sin \theta \left(-\omega_{x_1} \sin \phi \sin \theta \frac{\partial h}{\partial \theta} + \omega_{x_2} \cos \phi \sin \theta \frac{\partial h}{\partial \theta} - \omega_{x_1} \cos \phi \cos \theta \frac{\partial h}{\partial \phi} - \omega_{x_2} \sin \phi \cos \theta \frac{\partial h}{\partial \phi} \right. \\ & \quad \left. + \omega_{x_3} \sin \theta \frac{\partial h}{\partial \phi} + 2 \sin \theta \frac{\partial h}{\partial t} \right) \end{aligned} \quad (11)$$

If the axes are shifted, and the $x_1 - x_3$ plane lies in the horizontal position with x_2 in the vertical direction, last equation can be simplified with rotation about the x_3 axis, to

$$\sin \theta \frac{\partial}{\partial \theta} \left(G(h) \sin \theta \frac{\partial p}{\partial \theta} \right) + \frac{\partial}{\partial \phi} \left(G(h) \frac{\partial p}{\partial \phi} \right) = 6\mu R^2 \sin^2 \theta \left(\omega_{x_3} \frac{\partial h}{\partial \phi} + 2 \frac{\partial h}{\partial t} \right) \quad (12)$$

Treating θ and t as constants it is found that,

$$\frac{\partial}{\partial \phi} \left(G(h) \frac{\partial p}{\partial \phi} \right) = 6\mu R^2 \sin^2 \theta \left(\omega_{x_3} \frac{\partial h}{\partial \phi} \right)$$

$$\frac{\partial}{\partial \phi} \left(\left(h^3 + 3\sigma^2 h + 3\alpha^2 h + 3\alpha h^2 + 3\sigma^2 \alpha + \alpha^3 + \varepsilon \right) \frac{\partial p}{\partial \phi} \right) = 6\mu R^2 \sin^2 \theta \left(\omega_{x_3} \frac{\partial h}{\partial \phi} \right)$$

The dimensionless form of the above equation becomes,

$$\therefore \frac{\partial}{\partial \bar{\phi}} \left((1 + 3\bar{\sigma}^2 + 3\bar{\alpha}^2 + 3\bar{\alpha} + 3\bar{\sigma}^2\bar{\alpha} + \bar{\alpha}^3 + \bar{\varepsilon}) \frac{\partial \bar{p}}{\partial \bar{\phi}} \right) = 6 \sin^2 \theta \omega_{x_3} \quad (13)$$

where, $\bar{\sigma}$ = standard deviation in dimensionless form,

$\bar{\alpha}$ = variance in dimensionless form,

$\bar{\varepsilon}$ = skewness in dimensionless form,

\bar{p} = pressure in dimensionless form,

θ = non-dimensional rotation.

Thus the dimensionless boundary conditions are,

$$\bar{P} = 0 \quad \text{at } \bar{\phi} = 2\pi \quad (14)$$

$$\bar{P} = \omega_{x_3} \sin \theta \quad \text{at } \bar{\phi} = \pi$$

Integration of (13) in view of (14) leads to the expression for non-dimensional pressure distribution

$$\therefore \bar{P} = \frac{3 \sin^2 \theta \omega_{x_3}}{(1 + 3\bar{\sigma}^2 + 3\bar{\alpha}^2 + 3\bar{\alpha} + 3\bar{\sigma}^2\bar{\alpha} + \bar{\alpha}^3 + \bar{\varepsilon})} (\bar{\phi}^2 - 4\pi\bar{\phi} + 3\pi^2) + \omega_{x_3} \sin \theta \quad (15)$$

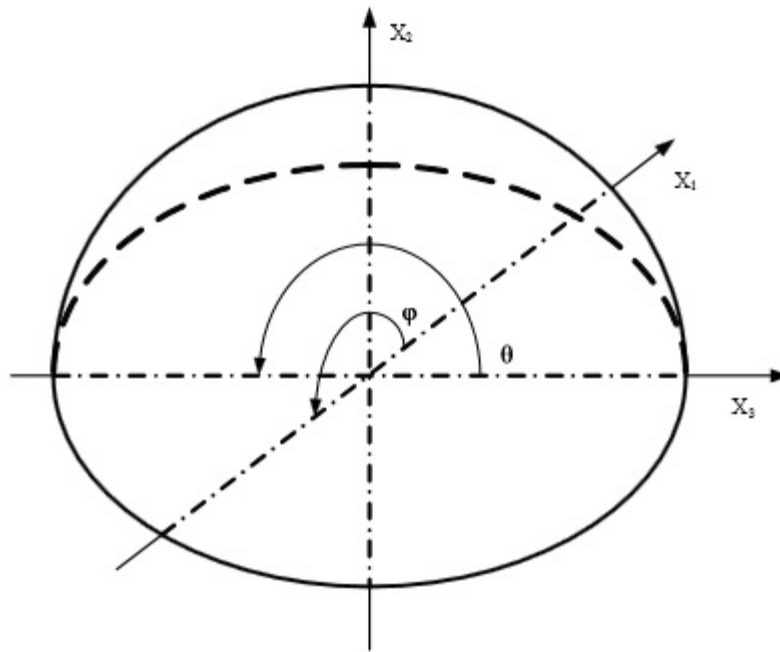


Fig. 1. Hemispherical shell on rotated axes

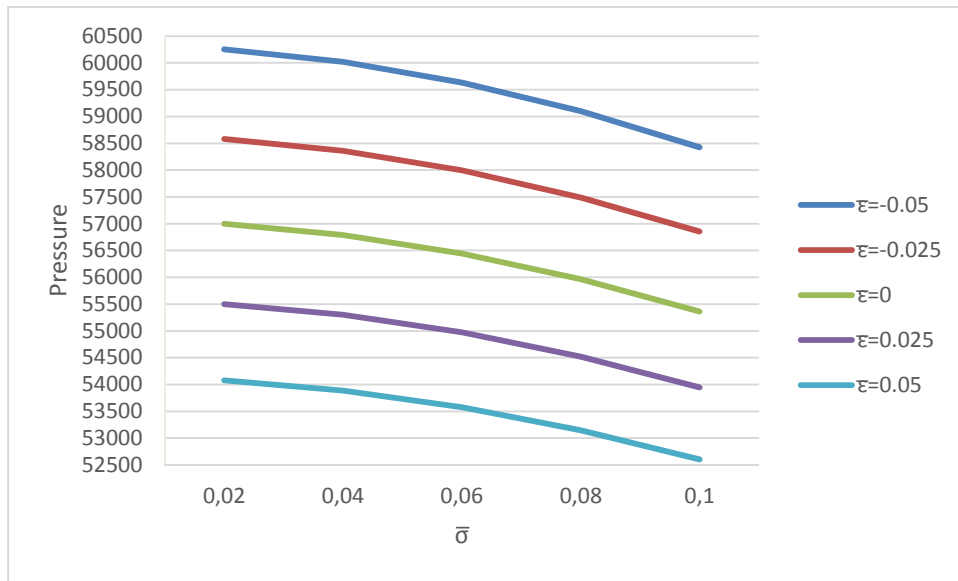


Fig. 2. Variation of Pressure distribution with respect to $\bar{\sigma}$ and $\bar{\epsilon}$

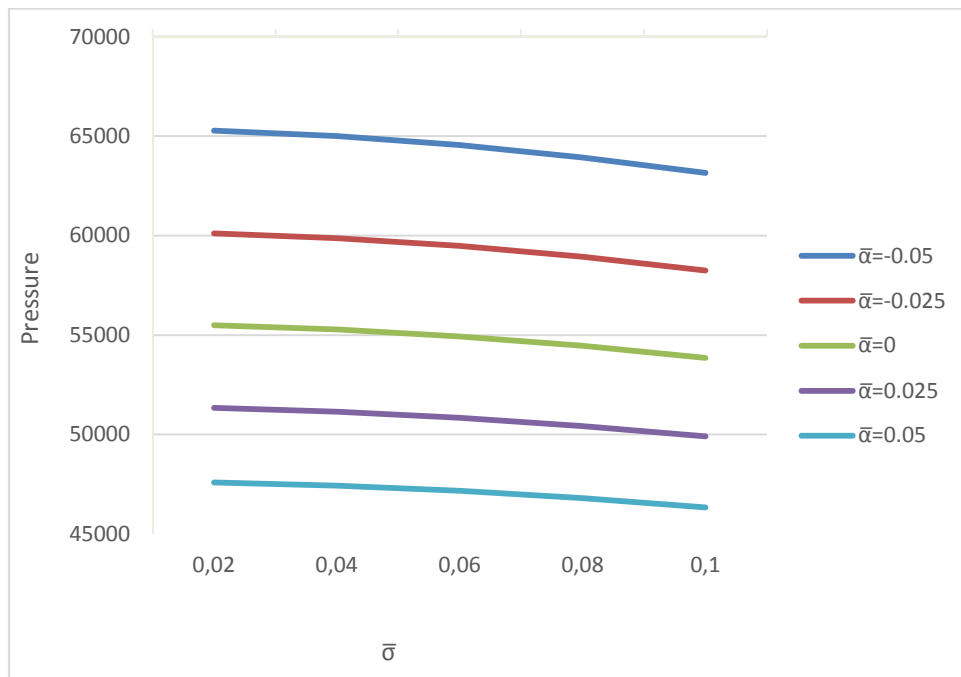


Fig. 3. Variation of Pressure distribution with respect to $\bar{\sigma}$ and $\bar{\alpha}$

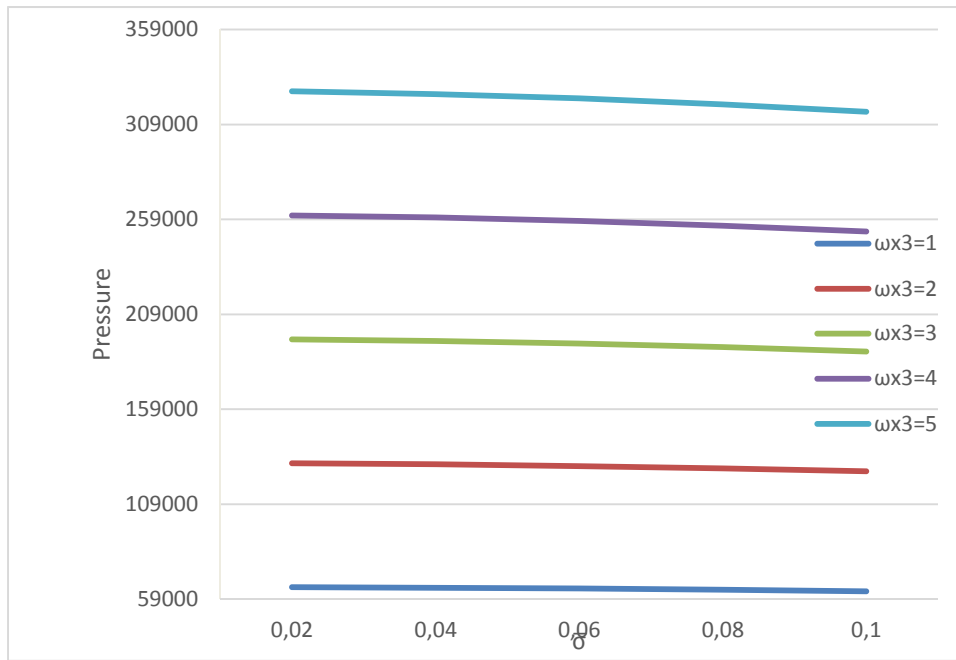


Fig. 4. Variation of Pressure distribution with respect to $\bar{\sigma}$ and ω_{x_3}

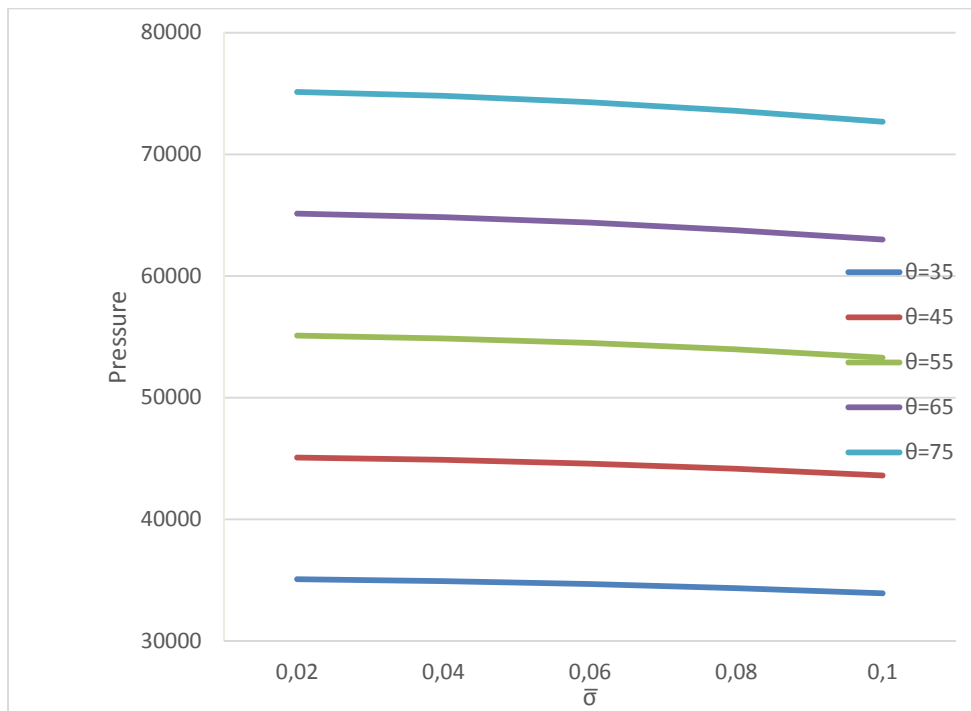


Fig. 5. Variation of Pressure distribution with respect to $\bar{\sigma}$ and θ

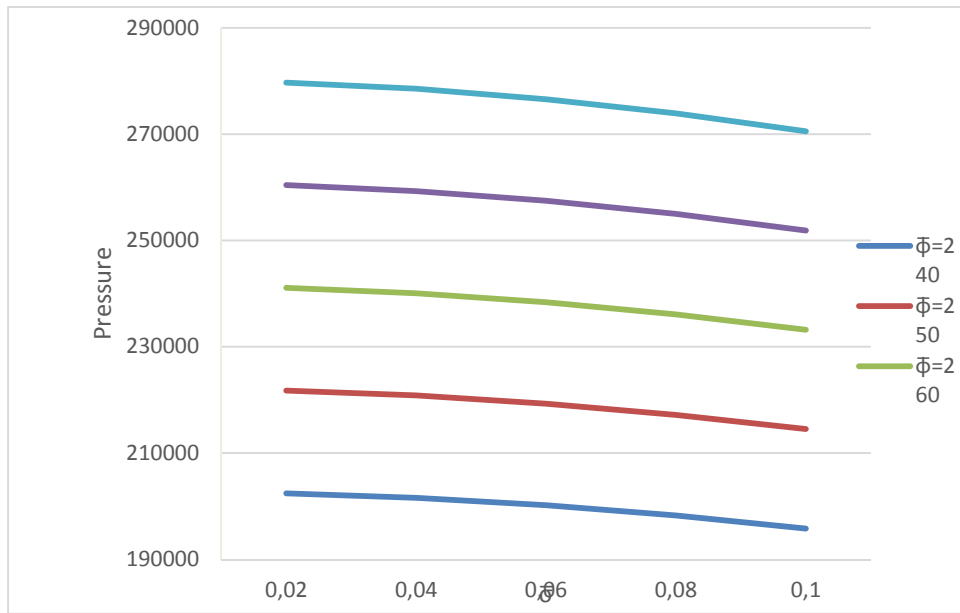


Fig. 6. Variation of Pressure distribution with respect to $\bar{\sigma}$ and $\bar{\phi}$

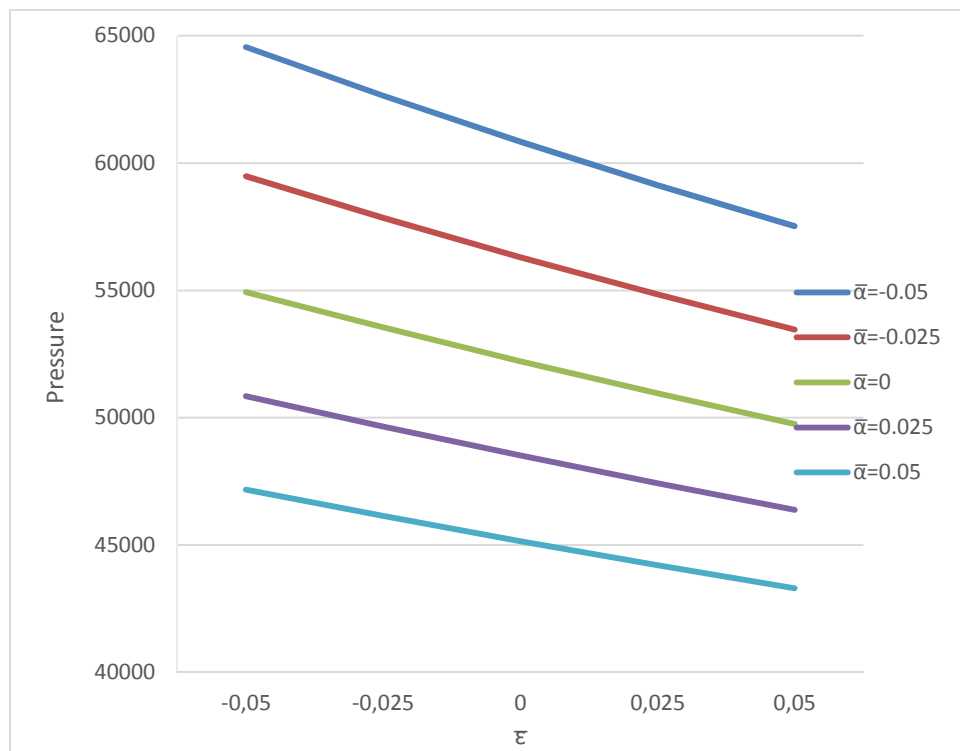


Fig. 7. Variation of Pressure distribution with respect to $\bar{\epsilon}$ and $\bar{\alpha}$

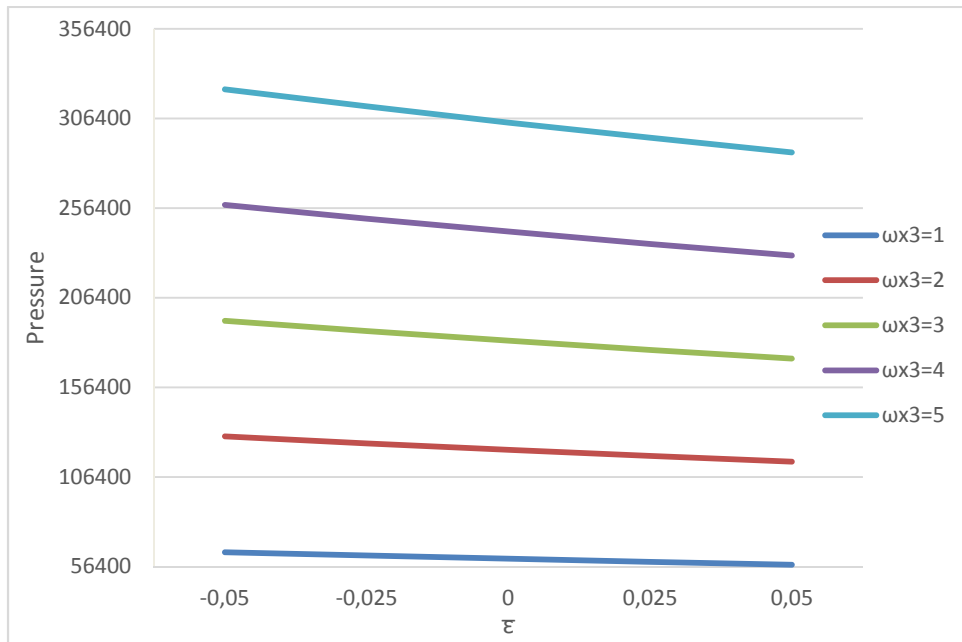


Fig. 8. Variation of Pressure distribution with respect to $\bar{\varepsilon}$ and ω_{x_3}

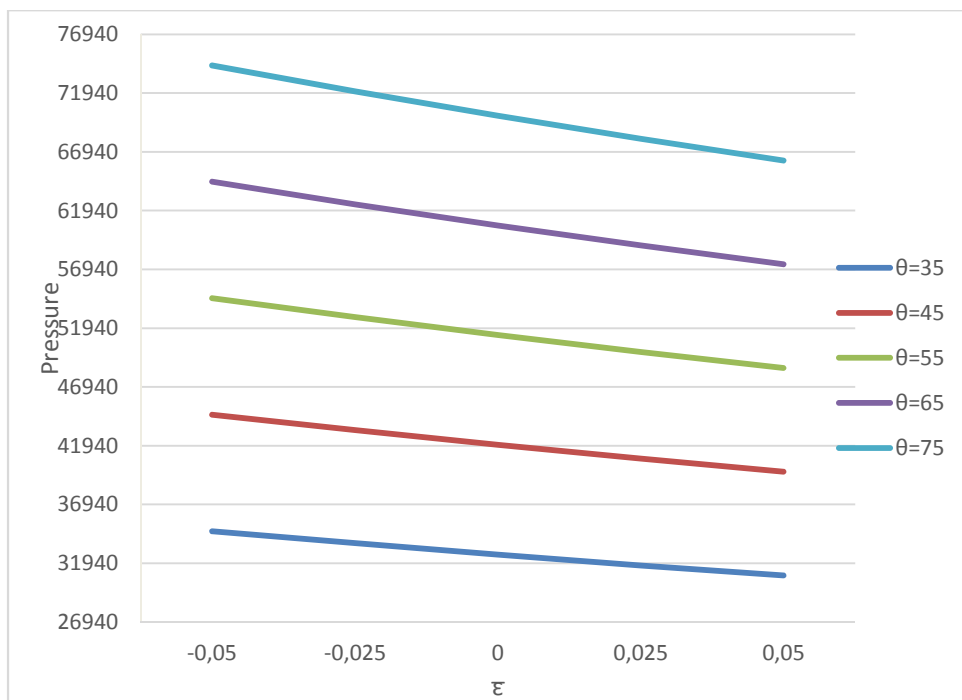


Fig. 9. Variation of Pressure distribution with respect to $\bar{\varepsilon}$ and θ

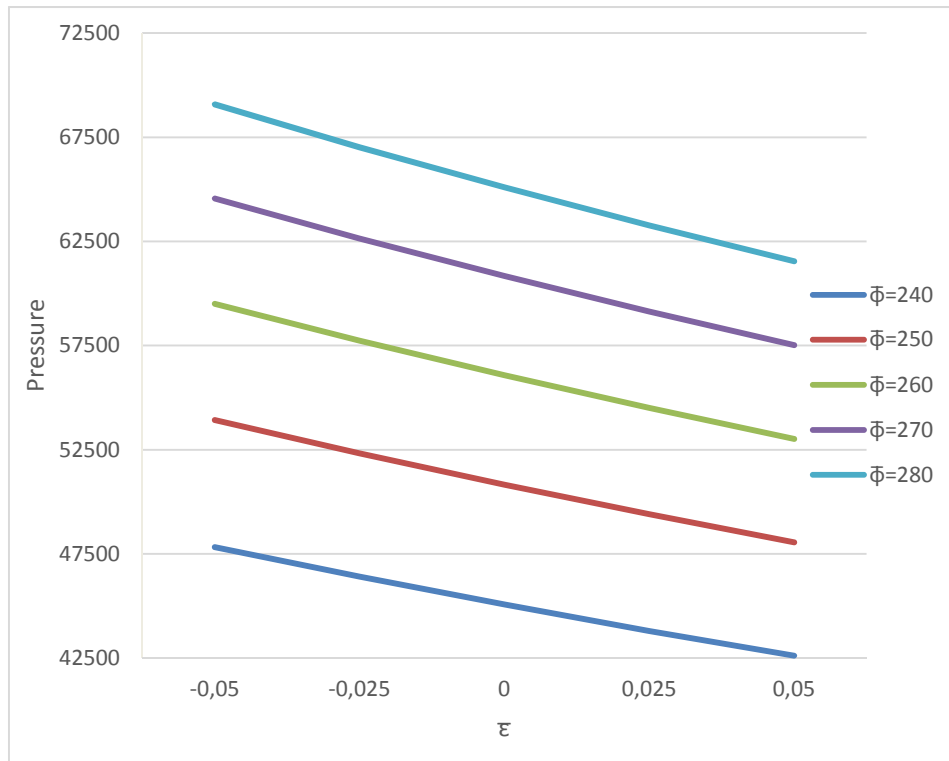


Fig. 10. Variation of Pressure distribution with respect to $\bar{\epsilon}$ and $\bar{\phi}$

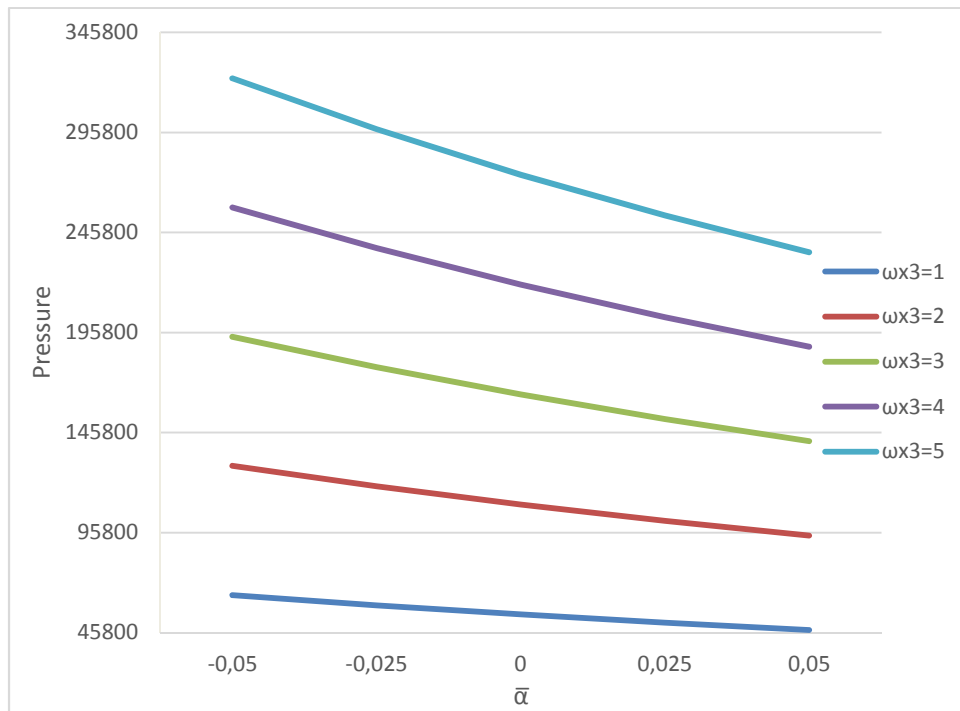


Fig. 11. Variation of Pressure distribution with respect to $\bar{\alpha}$ and ω_{x_3}

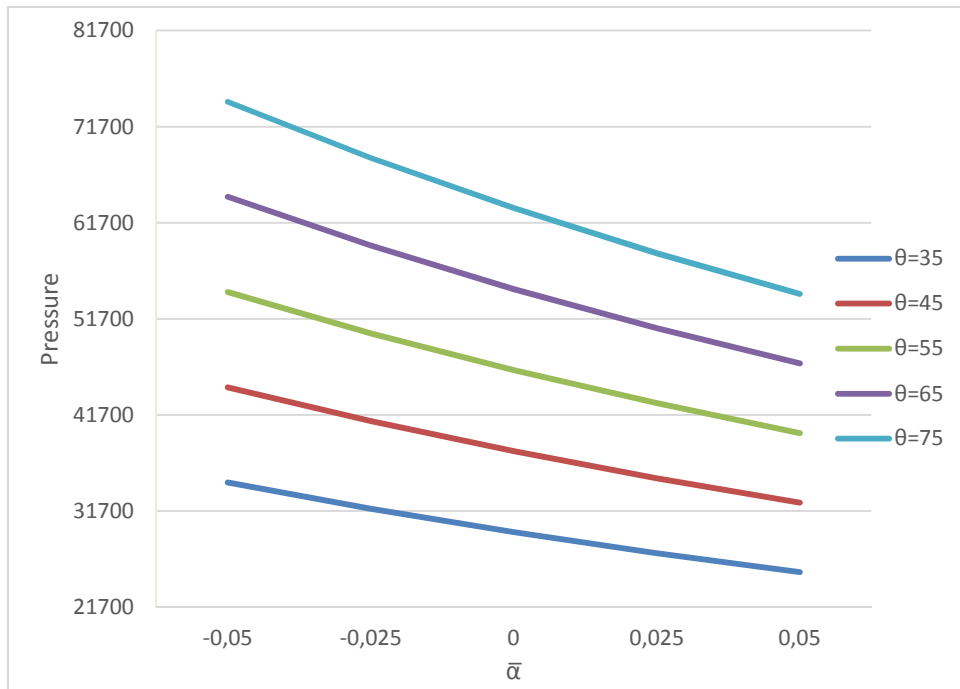


Fig. 12. Variation of Pressure distribution with respect to $\bar{\alpha}$ and θ

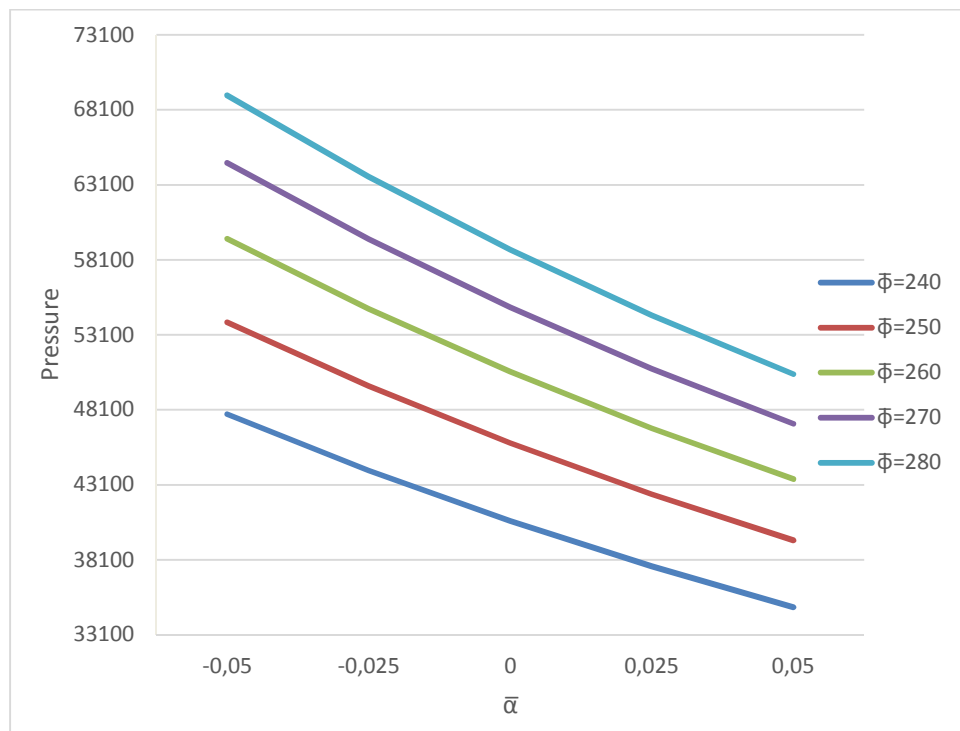


Fig. 13. Variation of Pressure distribution with respect to $\bar{\alpha}$ and $\bar{\phi}$

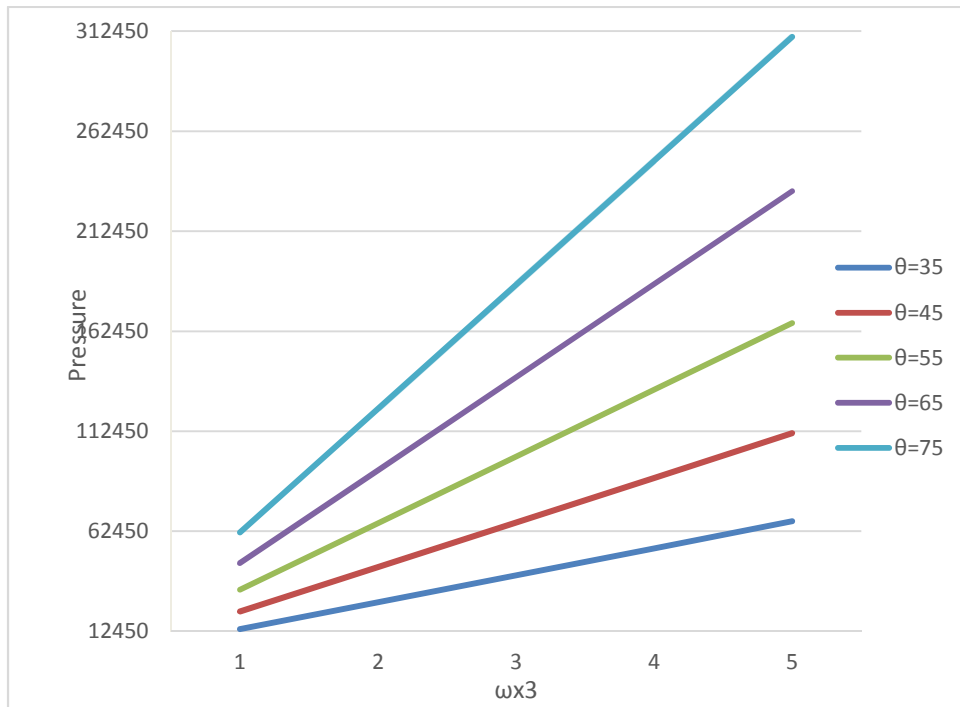


Fig. 14. Variation of Pressure distribution with respect to ω_{x_3} and θ

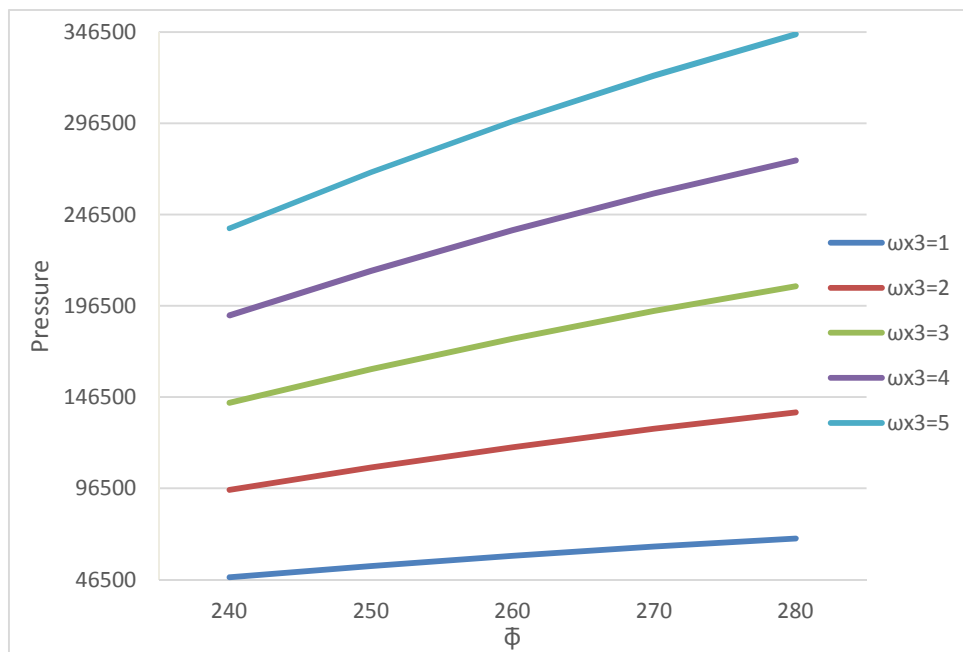


Fig. 15. Variation of Pressure distribution with respect to ω_{x_3} and $\bar{\phi}$

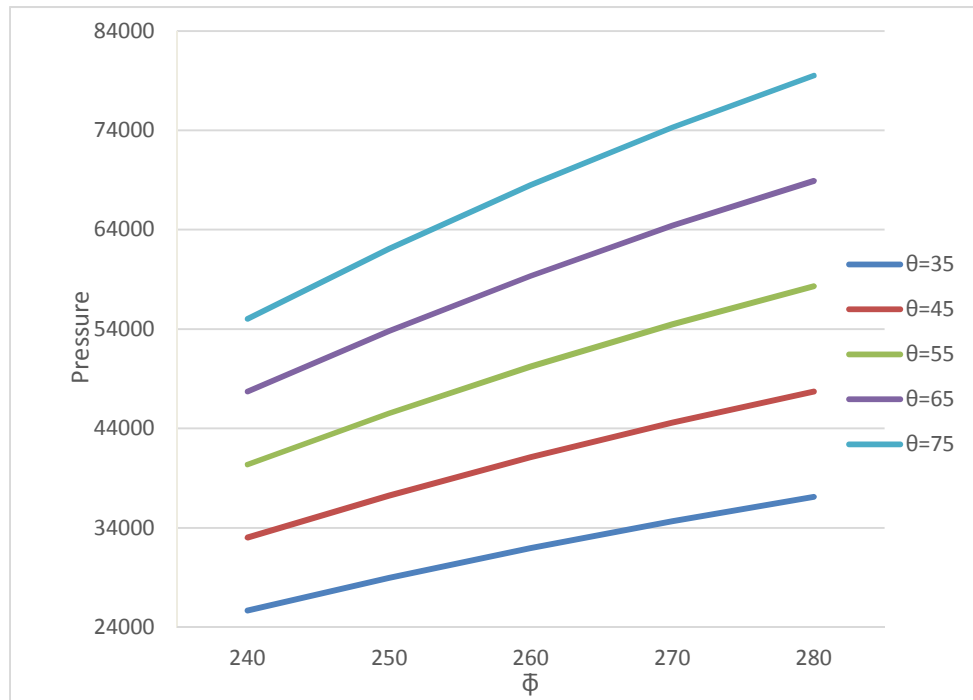


Fig. 16. Variation of Pressure distribution with respect to $\bar{\phi}$ and θ

3 RESULT AND DISCUSSION

It is clearly seen that the non-dimensional pressure distribution is determined from equation (15). The effect of standard deviation on the pressure profile can be seen from figures 2 to 6. It is observed that increase in standard deviation causes reduce pressures.

The fact that the negatively skewed roughness increases the pressure can be found from figures 7 to 10. However, positively skewed roughness decreases the pressure.

From figures 11 to 13 it is interesting to note that so far as the trends of pressure is concerned the variance follows the path of skewness. Therefore the variance (-ve) and negatively skewed roughness combined may have a significant role in enhancing the pressure distribution.

Lastly, the combined effect of ω_{x_3} and $\bar{\phi}$ becomes more significant as compared to ω_{x_3} and θ combine, as can be seen from figures 14 and 15.

4 CONCLUSION

This investigation can be modified to represent a rough hip-joint wherein different moments can be numerically analyzed. Further, this study makes it sure that the roughness aspects must be treated on a priority basis for smooth motion of the Hip-joints.

REFERENCES

- [1] Peeyush Chandra 'Mathematical models for synovial joints – A lubrication biomechanical study' PhD thesis , Department of Mathematics, Indian Institute of Technology, Kanpur,India,1975.
- [2] D .Dowson and V. Wright, Bio-tribology, in The Rheology of Lubricants, ed. T. C. Davenport, Applied Science Publishers, Barking, 1973, pp. 81-88
- [3] Z M Jin, D Dowson, J Fisher 'Analysis of fluid film lubrication in artificial hip joint replacements with surfaces of high elastic modulus'.Journal of Engineering Medicine.1997; Volume 211, Issue 3, Pages 247-256.

- [4] Feng Liu, Zhongming Jin, Paul Roberts, Peter Grigoris 'Effect of bearing geometry and structure support on transient elasto-hydrodynamic lubrication of metal-on-metal hip implants'. *Journal of Biomechanics*. 2007; Volume 40, Issue 6, Pages 1340–1349.
- [5] Qingen Meng, Leiming Gao, Feng Liu, Peiran Yang, John Fisher, Zhongmin Jin 'Contact mechanics and elasto-hydrodynamic lubrication in a novel metal-on-metal hip implant with an aspherical bearing surface'. *Journal of Biomechanics*. 2010; Volume 43, Issue 5, Pages 849–857.
- [6] L. Mattei, F. Di Puccio, B. Piccigallo, E. Ciulli 'Lubrication and Wear modelling of artificial hip joints: A review'. *Tribology International*. 2011; Volume 44, Issue 5, Pages 532-549.
- [7] Robert Sonntag, Jörn Reinders, Johannes S. Rieger, Daniel W. W. Heitzmann, J. Philippe Kretzer 'Hard-on-Hard Lubrication in the Artificial Hip under Dynamic Loading Conditions'. *Plos One*. 2013; Volume 8, Issue 8, e71622.
- [8] Francesca Di Puccio and Lorenza Mattei 'Biotribology of artificial hip joints'. *World J Orthop*. 2015; Volume 6, Issue 1, Pages 77-94.
- [9] Shatish Ramjee 'Numerical Analysis of Lubrication in an Artificial Hip Joint' PhD thesis, Department of Chemical Engineering, University of Pretoria, Pretoria, 2008.
- [10] Christensen H. and K. Tonder, 'The hydrodynamic lubrication of rough bearing surfaces of finite width'. *Journal of Tribology* 93.3 (1971): 324-329.
- [11] Christensen H. and K. Tonder, 'The hydrodynamic lubrication of rough journal bearings'. *Journal of Tribology* 95.2 (1973): 166-172.
- [12] Tonder K. and H. Christensen 'Waviness and roughness in hydrodynamic lubrication'. *Proceeding of the Institution Mechanical Engineers* 186.1 (1972): 807-812.
- [13] Bergmann, G.; Kneggenndorf, H.; Graichen, F. and Rohlmann, A. 'Influence of shoe and heel strike on the loading of a hip joint', 1995 *Journal of biomechanics*, Volume 28 Issue 7.